Water and Solute Transport Across Cellulose Acetate Membranes in the Treatment of Soybean Whey by Reverse Osmosis

E. C. BAKER, G. C. MUSTAKAS, M. D. MOOSEMILLER, and E. B. BAGLEY, *Northern Regional Research Center, Agricultural Research, Science and Education Administration, U.S. Department of Agriculture, Peoria, Illinois 61604*

Synopsis

In processing full-fat soy flour to produce an acid-precipitated lipid protein concentrate, there results a by-product whey fraction which, because of its high biological oxygen demand, represents a serious disposal problem. Processing of food waste streams by reverse osmosis has received considerable attention because of its low theoretical energy requirement, since no phase change is involved. A series of statistically designed and analyzed experiments were conducted on a pilot-plant reverse osmosis unit to study the effect of the operating parameters on solute and solvent transport in cellulose acetate membranes. Sucrose and sodium chloride solutions were tested in addition to soybean whey to relate the mixed solute system in whey to that of single-solute organic and inorganic feed solutions. Water flux was shown to have an Arrhenius dependency on temperature, and some membrane compaction was observed with the more porous membrane. Concentration polarization for sucrose and sodium chloride solutions increased linearly with water flux. Solute flux for soybean whey solutions decreased with molarity and was independent of pressure, whereas solute rejection increased with temperature and pressure and was independent of molarity. Good agreement was obtained using the derived parameters A, B, and π for soy whey in the diffusion transport model when compared to the observed experimental values.

INTRODUCTION

In processing full-fat soy flour to obtain an acid-precipitated lipid protein concentrate (LPC) curd,[1] an earlier development of this laboratory, a whey by-product results that contains soluble oligosaccharides and other whey solids. Because of its high biological oxygen demand (BOD), it represents a serious disposal problem.

Membrane processing in the forms of reverse osmosis and ultrafiltration provides a new technology for solving pollution problems in food processing wastes. One of the more attractive aspects of reverse osmosis is its low theoretical energy requirement, since no phase change is involved as in evaporation or drying. Reverse osmosis has become one of the major separation processes in less than two decades, mainly because of the impetus supplied by the Office of Saline Water of the U.S. Department of the Interior in the pursuit of techniques for the desalination of sea water.[2–7] The discovery by Reid and Breton[8] of cellulose acetate as an effective membrane material for salt rejection, together with the demonstration by Loeb et al.[9] of high-flux cellulose acetate membranes, initiated this technological growth.

The objective of this study was to determine the separation capabilities of cellulose acetate membranes in the fractionation and concentration of soybean

Journal of Applied Polymer Science, Vol. 24, 135–145 (1979)

whey. More specifically, we needed to determine the pure water transport for each membrane as well as the mass transfer variables for sucrose, sodium chloride, and LPC whey aqueous solutions.

These data will be used in optimizing the processing variables in subsequent pilot-plant studies involving the soybean wheys from various sources, such as those resulting from the production of soybean concentrates and isolates.

MATERIALS AND METHODS

Materials

Feed solutions were distilled water, aqueous sodium chloride, or sucrose solutions and LPC whey solution whose composition is given in Table I. These comprised four distinct feed solutions: pure water, a reference inorganic solution, a reference organic solution, and a test solution of mixed solutes.

Analytical Methods

Feed solutions, as well as the permeate and concentrate streams from each run, were analyzed for total solids by evaporation on a stream bath. In addition, all sucrose solutions were analyzed using a direct reading refractometer; sodium chloride solutions were analyzed for sodium on a Varian 120 atomic absorption spectrophotometer. Duplicate total solid assays were run for all whey solutions. Data points for sodium chloride and sucrose densities, viscosities, and osmotic pressures over the range of concentrations and temperatures investigated were taken from several references,[10–13] and general expressions were developed. Whey viscosities were run on a Brookfield LVT with UL adaptor; densities were measured gravimetrically.

TABLE I
Composition of Soybean LPC Whey

Component	As-is basis, %	Freeze-dried basis, %
Protein (total nitrogen = NPN × 6.25)	0.08	6.2
Nonprotein nitrogen (NPN)	0.01	0.6
Ash	0.31	23.0
Crude fat	0.01	0.6
Dextrose	0.04	3.2
Sucrose	0.30	22.3
Raffinose	0.06	4.4
Stachyose	0.22	16.3
Others (by difference)	0.31	23.4
	1.34	100.0

EQUIPMENT AND PROCEDURE

Equipment

The reverse osmosis (R.O.) unit used in our experiments was the OSMO-3319 by Osmonics, Inc., Hopkins, Minnesota (Fig. 1). The unit contains a cellulose acetate membrane, spiral wound to give a module with an effective area of 3.25 m^2 (35 sq. ft). The module was housed in a 10.2-cm (4-in.) I.D. pressure vessel 76 cm (2½ ft) long. A staged centrifugal pump developed 12.6 atm (185 psig) pressure. Two modules were supplied with the unit. One was rated at 97% NaCl rejection and the other, at 89%, with feed solution containing 1000 ppm NaCl at 25°C and 27.2 atm (400 psig). A cartridge prefilter completed the unit.

The feed tank was an agitated 113-l (30-gal) stainless-steel jacketed kettle. A booster pump was installed between the feed tank and the centrifugal pump to obtain operating pressures up to 15 atm (220 psig). Temperature was adjusted and controlled by flow through an Alfa-Laval plate heat exchanger serviced by hot water and a Borg–Warner brine chiller.

Procedure

Pure-water permeation rates at various operating temperatures and pressures were determined for the modules before running them on test solutions. This provided a bench mark for determining when the modules were adequately rejuvenated after a test run. Cleaning was generally discontinued when the modules regained 95% or more of their standard water rate.

Feed solution was pumped to the module, with the permeate and concentrate streams being returned to the feed tank. Since nothing was removed from the system except the samples for analysis, the feed concentration was held constant.

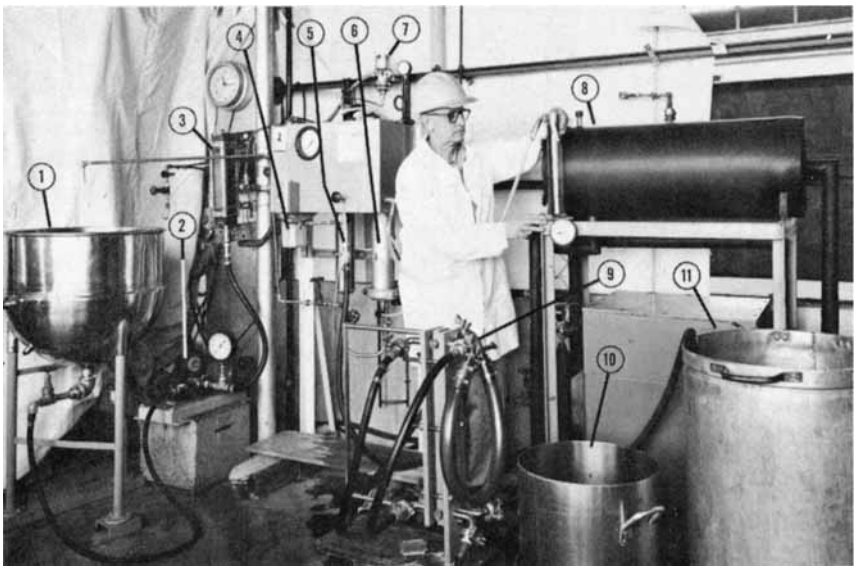

Fig. 1. Pilot plant reverse osmosis equipment: (1) feed tank, (2) booster pump, (3) flowmeter, (4) prefilter, (5) staged centrifugal pump, (6) pressure vessel, (7) low-pressure safety switch, (8) brine chiller, (9) plate heat exchanger, (10) concentrate collector, (11) permeate collector.

With the system operating on total recycle, pressure and temperature were adjusted and controlled at the design operating conditions for the data point. Feed, concentrate, and permeate rates were measured at intervals until no significant differences were observed between successive readings. At this point samples were removed for analysis.

Experimental Design

The experimental design was a three-factor response surface design with replicate center points plus the axial points.[14] The independent variables were identified and coded as shown in Table II. The purpose of the central composite design was to determine the response surfaces of the solute and solvent mass transfer coefficients, as well as the solute rejection for each membrane. When the feed was distilled water, a two-factor central composite design was used.

RESULTS AND DISCUSSION

Solvent Flux

Tight membranes function as diffusive transport barriers where both solute and solvent migrate within the membrane. Earlier workers[15–18] have prepared mathematical models of the transport process in diffusive-type membranes. Two basic assumptions of the model are that uncoupled flow occurs for each species and that both solute and solvent migrate by molecular (Fickian) diffusion. For the solvent component it has been shown that its flux J_1 is given by

$$J_1 \simeq \frac{\overline{C}_1 D_1 \overline{V}_1}{RT} \frac{(\Delta P - \Delta\pi)}{t_m} \tag{1}$$

(All symbols are defined at the end of the paper.) Let

$$A = \frac{\overline{C}_1 D_1 \overline{V}_1}{RTt_m} = \frac{J_1}{\Delta P - \Delta\pi} \tag{2}$$

where A is the solvent permeability coefficient. The transmembrane hydraulic pressure drop ΔP was found to be essentially equal to the applied pressure, i.e., $\Delta P = P$; and when the feed was pure water, the osmotic pressure difference was zero and eq. (2) further simplified to

$$A = J_1/P \tag{3}$$

From a series of statistically designed experiments, A values were determined then subjected to multiple regression analysis to yield A values for each mem-

TABLE II
Test Variables

Variable	Range	Center point	Factorial points		Axial points	
		0	−1	+1	$-k$	$+k$
Operating pressure, psig	110–220	165	130	200	110	220
Operating temperature, °C	10–40	25	16	34	10	40
Feed molarity, m	0.1–0.5	0.3	0.18	0.42	0.1	0.5

brane. Best fits were obtained with log A values and reciprocal absolute temperatures:

$$\log A_{M\text{-}89} = -0.663 - 0.0085P - 1038.7/(T + 273) \quad (4)$$

$$\log A_{M\text{-}97} = -0.705 - 1150/(T + 273) \quad (5)$$

Equation (4) shows A to be both pressure and temperature dependent for the 89 module, while eq. (5), for the 97 module, shows a temperature dependence only. These equations do not necessarily characterize all cellulose acetate membranes of the indicated levels of NaCl rejection but only these modules tested in this study.

Effect of Temperature

It has been suggested by other workers[19–21] that A has an Arrhenius dependence on temperature, i.e.,

$$\log A = \log A_0 - E_a/2.3RT_a \quad (6)$$

where E_a is the activation energy for the permeation of water through cellulose acetate. A semilogarithmic plot of A values calculated from eq. (3) for each module resulted in straight lines (Fig. 2). The data points for the 89 module clearly indicate the existence of two parallel lines of equal slope at operating pressures of 110 and 220 psig. The activation energy was calculated for each module by setting the slope of each line equal to $-E_a/2.3R$ and solving for E_a. A value of 4754 cal/mole was calculated for the 89 module and of 5266 cal/mole for the 97 module. These values represent the activation energies for the permeation of water through the membranes and are a measure of the relative resistance of the individual membranes to water flux. These values approximate

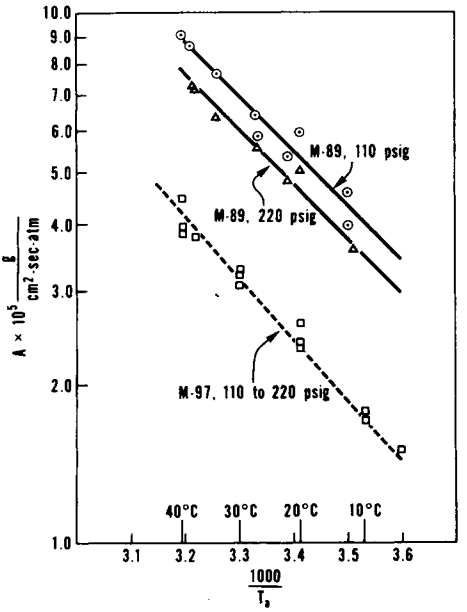

Fig. 2. Arrhenius dependence of A on temperature.

those reported by Lonsdale.[19] The intercept from the regression equations equals the constant A_0; then, for the 97 module,

$$A_{M\text{-}97} = 0.19724 \exp(-5266/RT_a) \tag{7}$$

The pressure dependence of the more porous 89 module is no doubt a manifestation of membrane compaction. Restating eq. (4),

$$\log A_{M\text{-}89} = \log 0.21727 - 0.0085P - 4754/2.3RT_a \tag{8}$$

$$= \log (0.21727/10^{0.0085P}) - 4754/2.3RT_a \tag{9}$$

Then

$$A_{M\text{-}89} = (0.21727/10^{0.0085P}) \exp(-4754/RT_a) \tag{10}$$

where 0.21727 = the constant $A_{0M\text{-}89}$ and $10^{0.0085P}$ is the membrane compaction factor.

Effect of Viscosity

Agrawal and Sourirajan found in their studies[15,22] with sodium chloride–water systems at 1500 psig that multiplying the product rate by the feed viscosity yields a function independent of temperature. Rearranging eq. (3),

$$J_1 = AP \tag{11}$$

and

$$J_1\eta = A\eta P \tag{12}$$

Viscosity also has an Arrhenius dependence on temperature, which can be demonstrated by a semilogarithmic plot of water viscosities versus reciprocal of absolute temperature (Fig. 3). By setting the slope of the viscosity line equal to $E/2.3R$ and solving for E, an activation energy of 4080 cal/mole was obtained for water. Then

$$\eta = \eta_0 \exp(E/RT_a) \tag{13}$$

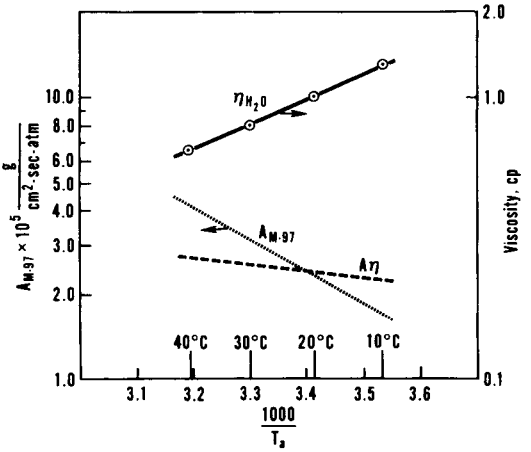

Fig. 3. Arrhenius dependence of A and η on temperature.

and solving for the constant η_0, a value of 0.000932 was obtained. From eq. (12) at a given pressure,

$$J_1\eta = A\eta = A_0 \exp(-E_a/RT_a)\eta_0 \exp(E/RT_a) \quad (14)$$

$$= A_0\eta_0 \exp[(E - E_a)/RT_a] \quad (15)$$

which shows that $J_1\eta$ can only be constant when $E_a = E$. This is illustrated in Figure 3, which shows for the 97 module that the negative slope of A is not entirely canceled out by the positive slope of viscosity. The same can be said for the 89 module.

Polarization Concentration

In a typical high-solute rejection membrane, the proportion of water that permeates the membrane is considerably higher than the solute, causing a depletion of water molecules on the upstream side of the membrane and a corresponding enrichment of solute molecules at the membrane interface. This effect is called concentration polarization and has several negative consequences. First, the local solute concentration at the membrane surface is increased, which increases the solute flux and lowers solute rejection. Second, the osmotic pressure at the membrane–solution interface is increased, causing a decrease in water flux. The ratio of the solute concentration at the membrane surface to the solute concentration in the feed is called the polarization modulus, i.e.,

$$C_{2m}/C_{2f} = M \quad (16)$$

Inclusion of the polarization modulus in the equation for water flux gives

$$J_1 = A[P - (M\pi_f - \pi_p)] \quad (17)$$

or

$$M = \frac{P - (J_1/A) + \pi_p}{\pi_f} \quad (18)$$

Solute Flux

The solute flux J_2 is determined by

$$J_2 = B\Delta C_2 = B(C_{2f} - C_{2p}) \quad (19)$$

where B is the solute permeation coefficient and ΔC_2 is the difference in solute concentration across the membrane. The B values were calculated from eq. (19) for each of the three solutes studied in each module. By multiple regression, equations were developed for each situation (Table III). The B values were pressure independent in all cases. Soybean LPC whey manifested varying degrees of both temperature and molarity dependence.

Solute Rejection

Solute rejection r is defined as

$$r = \frac{\Delta C_2}{C_{2f}} = \frac{C_{2f} - C_{2p}}{C_{2f}} = 1 - \frac{C_{2p}}{C_{2f}} \quad (20)$$

TABLE III
Solute Flux Regression Coefficients

Dependent variable	Feed	Module	Intercept	Temperature T^2	mT
$B \times 10^6$	NaCl–H_2O	89	466.570	3.28	—
$B \times 10^6$	NaCl–H_2O	97	34.621	—	2.77
$B \times 10^6$	sucrose–H_2O	89	15.296	0.0207	—
$B \times 10^6$	sucrose–H_2O	97	1.336	0.00087	—
$B \times 10^6$	soy LPC–whey	89	15.220	0.0380	−2.502
$B \times 10^6$	soy LPC–whey	97	8.170	0.0022	−0.4309

Rejections were calculated by eq. (20), and multiple regression analysis yielded the following equations for rejection of soybean LPC whey:

$$r_{M\text{-}89} = 0.8786 - 0.0055(\text{wt. \%})^2 - 0.000049T^2 + 0.00279(\text{wt. \%})P \quad (21)$$

$$r_{M\text{-}97} = 0.7862 - 0.0465(\text{wt. \%}) + 0.0151T - 0.00026T^2 + 0.00306(\text{wt. \%})P \quad (22)$$

Osmotic Pressure of Soy LPC Whey

From examination of the concentration polarization data (Fig. 4), it becomes apparent that as J_1 approaches zero, the polarization modulus M approaches unity. Consequently, at low water flux rates,

$$M\pi_f - \pi_p \doteq \pi_f - \pi_p \doteq \Delta\pi \quad (23)$$

From eq. (2),

$$\Delta\pi = P - J_1/A \quad (24)$$

from the van't Hoff equation,

$$\pi = CRT_a/MW \quad (25)$$

where MW is the molecular weight of the solute,

$$\pi_f = C_{2f}RT_a/MW \quad (26)$$

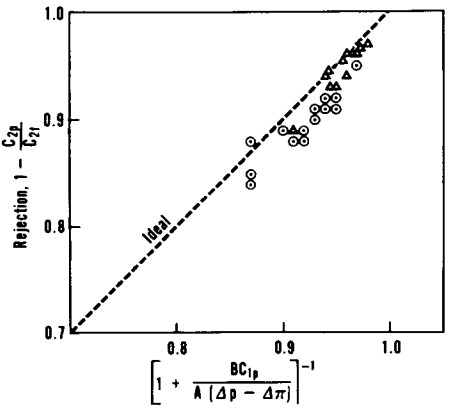

Fig. 4. Comparison of observed solute rejections with values predicted by the diffusion transport model: (⊙) M-89 whey; (△) M-97 whey.

and

$$\pi_p = C_{2p}RT_a/MW \tag{27}$$

where MW is the apparent molecular weight of the soy LPC whey. Then

$$MW = (RT_a/\Delta\pi)(C_{2f} - C_{2p}) \tag{28}$$

By selecting data points for soy LPC whey from the lower end of J_1 values where M approached unity for each module and by solving for $\Delta\pi$ values with eq. (24), an apparent MW for LPC whey of 139 was calculated.

From this, an expression for osmotic pressure of whey follows:

$$\pi_{\text{whey}} = CRT_a/139 \tag{29}$$

Mathematical Model for Soy LPC Whey

With the parameters A, B, and π for soy LPC whey defined, water flux and solute rejection can be calculated for any given set of operating conditions (i.e., temperature, pressure, and feed concentration). To test the mathematical model against observed experimental results, an equation containing all of the derived parameters was needed. By material balance on the downstream side of the membrane,

$$J_2/J_1 = C_{2p}/C_{1p} \qquad \text{or} \qquad C_{2p} = (J_2/J_1)C_{1p} \tag{30}$$

By eqs. (2), (19), and (20),

$$r = 1 - \frac{C_{2p}}{C_{2f}} = 1 - \frac{J_2}{J_1}\frac{C_{1p}}{C_{2f}} = \left[1 + \frac{BC_{1p}}{A[P - (\pi_f - \pi_p)]}\right]^{-1} \tag{31}$$

A plot of the observed rejection values versus eq. (31) shows a fairly good fit and reasonably accurate predictions of water flux and solute rejection are feasible using the derived parameters (Fig. 4).

Analyses were made by L. T. Black, J. D. Glover, and K. M. Rentfro. Pilot-plant equipment was operated by R. L. Brown. W. F. Kwolek helped in the experimental design and statistical evaluation. W. J. Bailey helped in processing data by the computer. The mention of firm names or trade products does not imply that they are endorsed or recommended by the U.S. Department of Agriculture over other firms or similar products not mentioned.

List of Symbols

A	solvent permeability coefficient, g/cm^2-sec-atm
A_0	solvent permeability constant, g/cm^2-sec-atm
B	solute permeability coefficient, cm/sec
$\overline{C}_1$	solvent concentration in the membrane, cm^3/cm^3
C	concentration, g/cm^3
D_1	diffusion coefficient of solvent, cm^2/sec
D_2	diffusion coefficient of solute, cm^2/sec
E	activation energy, cal/mol
E_a	activation energy of permeation of water, cal/mole
F	feed rate, g/cm^2-sec
J_1	solvent flux rate, g/cm^2-sec

J_2 solute flux rate, g/cm^2-sec
K solute distribution coefficient between membrane and solution
m molarity, moles/l.
M polarization modulus
MW molecular weight, g/mole
P applied hydraulic pressure, atm
ΔP hydraulic pressure drop across the membrane, atm
r solute rejection
R gas constant
t_m effective membrane thickness, cm
T_a absolute temperature of solution, °K
T temperature of solution, °C
$\overline{V}_1$ partial molar volume of water in solution, cm^3/mole
η viscosity, cp
η_0 constant, cp
π osmotic pressure, atm
$\Delta\pi$ osmotic pressure drop across the membrane, atm

Subscripts

1 solvent
2 solute
f feed
m membrane
p permeate

References

1. G. C. Mustakas, *Cereal Sci. Today*, **19**, 62 (1974).
2. Office of Water Research and Technology, R&D Report No. 76-15, Order No. PB 249818; *Study of Mass and Current Transfer in Membrane Processes*, U.S. Dept. of the Interior, 1976.
3. Office of Water Research and Technology, R&D Report No. 76-47, Order No. PB 253755; *Desalting Handbook for Planners, 1st ed.*, U.S. Dept. of the Interior, 1972.
4. Office of Saline Water, R&D Report No. 611, Order No. PB 198955; *Reverse Osmosis Desalting State-of-the-Art*, U.S. Dept. of the Interior, 1969.
5. Office of Saline Water, R&D Report No. 653, Order No. PB 202523U; *Water Transport in Hyperfiltration Membranes*, U.S. Dept. of the Interior, 1971.
6. Office of Saline Water, R&D Report No. 577, Order No. PB 200596; *Research on Improved Reverse Osmosis Membranes*, U.S. Dept. of the Interior, 1970.
7. Office of Water Research and Technology, R&D Report No. 76-14, Order No. PB 249743; *Structure of Reverse Osmosis Membranes*, U.S. Dept. of the Interior, 1976.
8. C. E. Reid and E. J. Breton, *J. Appl. Polym. Sci.*, **1**, 133 (1959).
9. S. Loeb, S. Sourirajan, and D. E. Weaver, U.S. Pat. 3,133,137, May 12, 1964.
10. F. J. Bates and Associates, *Polarimetry, Saccharimetry and the Sugars*, Circular of the National Bureau of Standards, No. C440, U.S. G.P.O., Washington, D.C., 1942.
11. E. W. Washburn, Ed., *Iternational Critical Tables of Numerical Data, Physics, Chemistry and Technology*, McGraw-Hill, New York, 1928, IV.
12. C. A. Browne and F. W. Zerban, *Physical and Chemical Methods of Sugar Analysis*, Wiley, New York, 1941.
13. R. W. Stoughton and M. H. Lietzke, *J. Chem. Eng. Data*, **10**, 3 (1965).
14. G. E. P. Box and H. L. Lucas, *Biometrika*, **46**, 77–90 (1959).
15. S. Sourirajan, *Reverse Osmosis*, Academic, New York, 1970.
16. W. F. Blatt, A. Dravid, A. S. Michaels, and L. Nelson, in *Membrane Science and Technology*, J. E. Flinn, Ed., Plenum, New York, 1970, pp. 48–73.
17. C. E. Reid, in *Desalination by Reverse Osmosis*, U. Merten, Ed., M.I.T. Press, Cambridge, Mass., 1966, Chap. 1.

18. H. K. Lonsdale, in *Industrial Processing with Membranes,* R. E. Lacey and S. Loeb, Eds., Wiley–Interscience, New York, 1972, Chap. VIII.

19. H. K. Lonsdale, in *Desalination by Reverse Osmosis,* U. Merten, Ed., M.I.T. Press, Cambridge, Mass., 1966, Chap. 4.

20. T. K. Sherwood, P. L. T. Brian, R. E. Fisher, and L. Dresner, *Ind. Eng. Chem., Fundam.,* **4,** 113 (1965).

21. L. E. Monge, B. J. McCoy, and R. L. Merson, *J. Food. Sci.,* **38,** 633 (1973).

22. J. P. Agrawal and S. Sourirajan, *Ind. Eng. Chem., Process Des. Dev.,* **8,** 439 (1969).

Received July 18, 1978
Revised October 5, 1978